

Complexity and frequency hierarchies in the catfish retina

M. J. KORENBERG,¹ H. M. SAKAI² and K.-I. NAKA^{2,3}

¹Queens University, Department of Electrical and Computer Engineering, Kingston, Ontario, Canada

²NYU Medical Center, Department of Ophthalmology, 550 First Avenue, New York, NY 10016, USA

³NYU Medical Center, Departments of Biophysics, Physiology, 550 First Avenue, New York, NY 10016, USA

Received 21 November 1995; accepted 12 August 1996

Abstract—The intricate connectivity and interactions between neurons in the vertebrate retina have made their individual roles in signal processing very difficult to elucidate. We have used a recently developed mathematical tool, fast orthogonal search (FOS), to probe the catfish outer (distal) and inner (proximal) retina, and study the signal processing within. Through FOS, a given waveform can be decomposed into a parsimonious sinusoidal series containing the most significant constituent frequencies. In particular, we examined the light-evoked first-order Wiener kernels of horizontal cells and on-bipolar cells, and on-off, off- and on-amacrine and ganglion cells. Here we report a hierarchy (correlation coefficient up to 0.86) in preferred frequency and complexity of response corresponding to the retina's structural hierarchy. In addition, clear differences between on-, on-off and off-cell functional characteristics were detected. For example, the kernel waveform for the on-amacrine cell was found to be more complex and to have a higher preferred frequency than that for the off-amacrine cell. Indeed FOS analysis revealed that both off- (sustained) amacrine and off-ganglion cells exhibit significantly less complexity in their waveforms for signal processing of light input than do the corresponding on- and on-off cells. This shows a clear breakdown in symmetry between on- and off-pathways, and suggests that connections to off-cells may provide fewer or a smaller variety of inputs than those to on- and on-off cells. Many of our new findings can be appreciated by assuming an underlying cascade structure for the retinal information processing. The FOS findings in particular support the following previously advanced hypothesis: the transition in nonlinear processing from on-off amacrine to on- or off-amacrine cells is due to high-pass linear filtering. Furthermore, our results indicate that the high-pass filtering is more sharply differentiating for the on-amacrine than for the off-amacrine cell.

Key words: Kernel; cascade; spectral analysis; retina; network; catfish.

1. INTRODUCTION

In the vertebrate retina monotonous hyperpolarization (an analog process) produced in the receptors is progressively transformed culminating as a series of spike discharges (a point process) from the ganglion cells, the output stage of the retina. The transformations can be appreciated by observing, for example, the patterns of response evoked by step inputs, i.e. monotonous hyperpolarizing response in the receptor and horizontal cells versus transient and complex response from the amacrine and ganglion cells [1, 2]. Unravelling of the modes of such transformations and their quantitative definition have been problematic. Previous white-noise analysis has shown that the transformation involved at least two processes: (1) introduction of higher frequency components and (2) generation of static nonlinearity [3–7].

Korenberg [8, 9] has lately developed an analytical procedure, fast orthogonal search (FOS), enabling concise information concerning frequency content and complexity to

be readily measured from time-series data. Through FOS, a given time series is decomposed into a parsimonious sinusoidal series representation containing only the most significant constituent frequencies, which are not necessarily commensurate. We have applied this method to analyze the hierarchical nature of the neuronal network in penetrating from outer to inner retina to show quantitatively: (1) neurons progressively become capable of responding to faster signals and (2) response complexity increases, with the response of on-center and on-off cells being more complex than that of off-center cells.

More generally, we have been able to systematically group the neurons into graded orders, both for the preferred frequencies of the response and for the relative response complexity. Because we have found these series of groupings of the neurons, we refer to the arrangements as frequency and complexity hierarchies.

2. MATERIALS AND METHODS

Experiments were all conducted on the eye-cup preparation of channel catfish, *Ictalurus punctatus*, at the National Institutes of Basic Biology, Okazaki, Japan. Responses were all evoked by a field of light modulated by Gaussian white-noise, with a mean luminance of $30 \mu\text{W}/\text{cm}^2$. The other experimental parameters were kept as constant as possible. Further details of experimental procedures are available [3, 6]. The representative first-order Wiener kernels for 44 preganglionic neurons and 32 ganglion cells were selected from a library of kernels compiled during the last few years.

2.1. List of abbreviations

H cell or kernel	the (cone) horizontal cell or its first-order kernel.
BA cell or kernel	the on-center bipolar cell or its first-order kernel.
C cell or kernel	the C (on-off transient) amacrine cell or its first-order kernel.
NA and NB cell or kernel	the NA (sustained depolarizing or on-center) and NB (sustained hyperpolarizing or off-center) amacrine cell or their first-order kernels.
GA, GB and GC cell or kernel	the on-, off-center and on-off ganglion cells or their first-order kernels.

3. ANALYTICAL METHODS

3.1. Some features of FOS analysis

The first-order Wiener kernels were obtained by cross-correlating the white-noise modulated light input against the resulting neuronal response. Roughly speaking, the first-order kernel is the response of the best linear approximation of the system to a brief flash superposed on a steady (constant) luminance. In past studies, several kernel parameters such as peak response time or amplitude have been extracted. In addition, direct observation of a kernel's waveform gives an impression of frequency response characteristics. However, a kernel, a time-domain representation, has to be transformed into the frequency domain to extract detailed frequency characteristics. In linear system theory, an impulse response can be transformed into a frequency response via the Fourier transform and vice versa. In this paper we will characterize the kernels by decomposing them into discrete sinusoids by use of FOS analysis. Here we briefly illustrate some of the features of FOS analysis which are used below.

In brief, FOS approximates a given time-series by a concise sinusoidal series model, comprising a sum of sine and cosine terms. In the obtained model, the frequencies and coefficients of the sine and cosine terms are *nearly* least-square estimates, i.e. estimates minimizing the mean-square error between the time-series data and the model. We say 'nearly' because the frequencies are selected from a finite set of candidates and because the selection is suboptimal with the frequencies selected sequentially. Once the frequencies have been selected by FOS, an iterative procedure [10, 11] can be used to converge toward the least-square estimates. However, extensive testing on noisy data [9–11] has shown FOS to be highly accurate even without iteration. The frequency resolution of FOS is generally significantly finer [9] than that of the discrete Fourier transform (DFT). Other algorithms for error minimization, e.g. the Levenberg–Marquardt method [12] can also be used. However, deterministic techniques, of which the Levenberg–Marquardt method is an example, can converge very slowly when fitting oscillatory waveforms and may then have convergence problems when a large number of parameters (more than 10) are to be determined or they may 'get stuck' in a local minimum. Stochastic techniques do not become mired in local minima but are very slow. While FOS is deterministic, it is particularly good in sinusoidal analysis at rapidly locating the true minimum region even when many parameters (e.g. 31 or more) need be determined.

Figure 1 compares results obtained by the classical DFT with FOS analysis of an NB kernel. Figure 1A shows the frequency response gain plot obtained from DFT analysis of the 128-point light-evoked first-order Wiener kernel, the given time-series data. The frequency response is bandpass and the peak frequency appears to be about 20 Hz, but there is considerable spread in the plot. Frequency resolution is about 4 Hz, actually 1/128 times the sampling frequency of 500 Hz. The FOS economy of representation is illustrated in Fig. 1B–D. These show, in the time-domain, the first 100 points of the actual kernel together with the best-fits attained (to the 128 point kernel) using the most significant three, seven and 11 sinusoidal components, respectively. The 11-frequency fit achieved a mean-square error (MSE) of less than

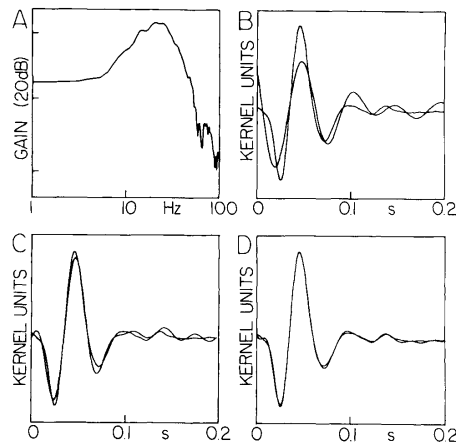


Figure 1. Comparison of DFT and FOS analyses of a first-order Wiener kernel, illustrated by an off-center sustained-amacrine cell (NB). All kernels analyzed in the present study actually comprised 128 data points but only the first 100 points are shown here and in subsequent figures. (A) Gain plot from DFT. (B)–(D) Successive FOS fits to the kernel using the ‘best’ three, seven and 11 sinusoidal frequencies. The MSE for (D) is $< 0.3\%$. Most NB cells studied could be accurately represented (MSE $< 0.5\%$) by about eight sinusoidal components.

0.3% of the time-series variance. (This cell is somewhat atypical: most NB cells we studied could be accurately represented using about eight sinusoidal components.) The key frequencies were chosen by systematically searching, in 0.5 Hz increments, 100 candidate frequencies up to 50 Hz. The same sampling rate (500 Hz) and set of candidate frequencies were used throughout this work. The preferred (i.e. the first) frequency selected in this example was 18.5 Hz.

Thus FOS analysis allows us to define (in addition to other measures):

- (1) The preferred frequency, i.e. the single sinusoidal frequency providing the best-fit, in the least-square sense, to the kernel.
- (2) The MSE remaining after approximating a kernel by a given number of the most significant sinusoids.
- (3) The number of sinusoids required to reproduce a kernel waveform to within a given degree of accuracy.

The first measure gives us an estimate of frequency response characteristics, and the second and third measure the degree of complexity of a kernel waveform.

More precisely, in this paper we studied, among other things, the complexity of first-order Wiener kernel waveforms measured by the percent mean-square error remaining after FOS had found the best 3- or 4-sinusoid fit (the 3f- or 4f-MSE). Another index of complexity used was the number of sinusoids selected until the process automatically

terminated (because no further choice could reduce the mean-square error by more than 0.2% of the time-series variance). Employing the 0.2% threshold as a stopping criterion almost invariably resulted in a sinusoidal series fitting the kernel to considerably better than 99% variance accounted for. The three measures of complexity are strongly correlated. Over the 44 preganglionic neurons in our first study, there was a correlation of 0.614 between the number of sinusoids selected and the 4f-MSE, for a level of significance better than 0.001 (i.e. $P < 0.001$). The correlation between the number of sinusoids selected and the 3f-MSE was 0.571 ($P < 0.001$), and the correlation between 3f- and 4f-MSE was 0.9388 ($P < 10^{-7}$).

In our studies of 44 preganglion and 32 ganglion cells, FOS appeared to be most sensitive in detecting differences in kernel waveform complexity using the total number of sinusoids selected test and the 4f-MSE test. The correlation between these two tests was 0.69 over the total sample of 76 neurons, significant at a level better than 10^{-6} .

Thus, the 3f- and 4f-MSE and total number of sinusoids selected tests are closely related and provide consistent measures. Nevertheless, the reader may question whether 'complexity' is an appropriate name for what these tests measure or whether 'broadbandedness of the spectrum' would be a more accurate term. For example, a pure delay element would have a flat (i.e. broadband) spectrum, so that FOS should select many significant frequencies and yet this element corresponds to a very simple system. However, the kernels we studied have two important characteristics which justify our use of 'complexity' to describe what the tests measure here. First, all kernels analyzed had no significant frequency content beyond 50 Hz. A spectrum that is flat only up to 50 Hz would correspond to a very complex waveform. Second, none of the kernels were of very brief duration; rather they had significant amplitude values for at least 50 samples. For such kernels, there was a clear correspondence between how complicated the waveforms appeared and the number of sinusoids selected (or the 3f- or 4f-MSE). For example, on-bipolar cells had obviously much simpler waveforms and required significantly fewer sinusoids for accurate approximation than NA cells. Figure 5 discussed below illustrates for ganglion cells the same correspondence between waveform complexity and these test measures. For these reasons, we have used 'complexity' to describe what the tests measure here, while recognizing that others may prefer to call it 'broadbandedness of the spectrum'. Notice that we are referring to the complexity of the kernel *waveform* and not of the corresponding system's functioning.

Finally, note that FOS is used herein to approximate the kernel itself and *not* its Fourier transform or transfer function, by a concise sinusoidal series representation defined over a finite record. Instead of this approach, we could have obtained another kind of representation by approximating the Fourier transform of each kernel by a rational expression, e.g. see the work of Fuortes and Hodgkin [13] and Shapley and Victor [14].

A central point of the present paper is that our complexity tests measure an intrinsic property of each cell. Nevertheless, it is worth noting that one limitation of the analysis in the form presented below is that it is sensitive to choice of interval length over which the kernel is defined. This is because it approximates kernels which decay with time

by a finite sum of sinusoids (which never die away). Due to this problem, each kernel is approximated by the sinusoidal series only over a finite interval, where the kernel assumes its non-negligible values. In the present paper, 128 point kernels were always used (with one exception which we will describe in the next paragraph). However, the choice of interval length will affect the values of the significant frequencies and amplitudes selected by FOS to approximate the kernels. This is because the longer the interval, the longer the decaying kernel tail which has to be approximated. One way around this problem is to replace the sinusoids by exponentially decaying sinusoids, since the latter functions can also be used in FOS to approximate time-series data [9]. The rate of exponential decay can be chosen by FOS but preferably would be fixed at *one* value for all the kernel records. Thus, the kernels would be approximated using functions which themselves have the property of decaying to zero as time increases, thereby reducing the dependence on interval length of the selected frequencies and amplitudes. Indeed, the tail of the kernel, which tends to be noisier data, would have much less effect on the choice of frequencies and amplitudes.

Another way to investigate the sensitivity to kernel length is to repeat the analysis with a different choice of interval over which the kernel is defined. To do this, we appended 256 zeros at the end of our 128 point ganglion cell kernels, so that each of the amended kernels now comprised 384 points. There was very little, and certainly no systematic change in the preferred frequencies for the amended kernels as compared to the original kernels. The amended kernels did have significantly increased complexity: approximately double on the measure we investigated, the ‘number of sinusoids selected’ test. However, the *relative* complexities of the off-center, on-center and on-off ganglion cells did not change for the amended kernels, and this is the important point. Indeed, none of our conclusions concerning the preferred frequency or relative complexity were altered despite increasing the interval length to three times longer than used previously. For this reason, one fixed length, covering 128 points, was used in the rest of our paper for each of our kernels.

3.2. Example

Figure 2 shows the first 100 points of the first-order Wiener kernel measured for an off-center (GB) ganglion cell. Again, the sampling interval was 2 ms, for a sampling rate of 500 Hz, and 128 kernel values were estimated. A Fourier series analysis of these kernel measurements is therefore, as noted above, limited to a resolution of $500/128 = 3.906$ Hz.

FOS approximates the kernel using a parsimonious sum of sinusoidal components. A key aspect of the algorithm is the use of an orthogonal framework to find efficiently the significant frequencies in the kernel. Each sinusoidal component which is found has the form:

$$z_i(t) = A_i \sin \omega_i t + B_i \cos \omega_i t. \quad (1)$$

Here ω_i is the frequency of the i th sinusoid, and A_i and B_i are the corresponding sine and cosine coefficients (or ‘amplitudes’), respectively. The approximation of the kernel also uses a constant term.

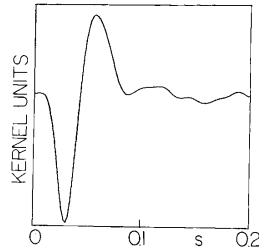


Figure 2. First-order Wiener kernel for an off-center (GB) ganglion cell.

Table 1.

FOS analysis of first-order Wiener kernel of the off-center ganglion cell kernel of Fig. 2 (frequencies are listed in order of estimation, MSE = 0.347%, constant = 91.339)

Frequency (Hz)	Sine amplitude	Cosine amplitude
14.5	-69.133	128.588
15.0	5.235	-131.007
10.5	-22.528	16.003
5.5	-19.668	-12.420
21.5	-25.761	-0.309
23.0	13.826	-34.094
1.5	-96.494	-38.047
27.0	-1.104	-59.628
28.0	43.820	33.136
30.5	0.617	8.659

The frequencies ω_i are found by scanning a set of candidate frequencies $\omega_A, \omega_B, \dots$ and selecting those sinusoidal components most effective in reducing the MSE of approximating the kernel. The candidate frequencies are not required to be commensurate nor integral multiples of a fundamental frequency corresponding to the kernel length. To facilitate selection of frequencies, the sine and cosine pair at each candidate frequency are implicitly orthogonalized relative to each other as well as to all previously selected terms [9]. This simplifies the measurement of the potential reduction in MSE by choosing any particular sine and cosine pair, and the candidate frequency with the greatest reduction is selected at each stage. Once all of the frequencies ω_i have been chosen, the sine and cosine coefficients A_i and B_i can be readily calculated from the weights of orthogonalized selected terms through a recursive procedure [9]. For the kernel of Fig. 2, FOS analysis estimated the frequencies (and sine and cosine amplitudes) shown in Table 1 in their order of detection. (The constant estimated here, i.e. 91.339, is one to two orders of magnitude larger than those for the other off-center ganglion cells studied, which typically had a magnitude between 1 and 10.)

In this example, the FOS analysis automatically terminated after 10 frequencies were selected, because no remaining candidate frequency could reduce the MSE by more than 0.2% of the time-series variance. Note that in Table 1 the first frequency selected, 14.5 Hz, is the single frequency giving the smallest MSE fit to the kernel. As stated above, this frequency is referred to as the 'preferred frequency'.

The reader may notice that in Table 1, the amplitudes of the sinusoids start to increase after the fifth component (21.5 Hz). While this is not a common occurrence, it is not contradictory. The reader is reminded that the sinusoids selected are *not* orthogonal over the 128 point kernel length, so one cannot conclude simply from their amplitudes what their contributions are to reducing the MSE. Obviously, a measured kernel will show some variability from one estimate to another for the same neuron. This variability is due both to measurement noise and to deviations of the experimental input from ideal white Gaussian noise, in addition to small changes in the biological preparation itself. Clearly, such variability will affect the results of subsequent analysis by DFT, FOS or other methods. However, each kernel was measured using a lengthy experimental record to greatly reduce the variability between multiple estimates. Moreover, when FOS was applied to different kernel estimates of the same neuron, very similar results were obtained both for preferred frequency and complexity measures. Finally, sufficiently large samples of neurons were used to cope with the effects of such variability so that all FOS findings reported below achieved statistical significance, usually at a high level.

4. RESULTS

4.1. Preganglion cells

Our 44 cell sample comprised eight horizontal, seven on-bipolar, eight C amacrine, 10 NB amacrine and 11 NA amacrine cells. Statistically significant differences in preferred frequency and complexity were observed as follows.

4.4.1. Frequency hierarchy. We found a very pronounced frequency hierarchy, with the preferred frequency almost steadily increasing as we proceeded from the distal (outer) to proximal (inner) retina. Point biserial correlation revealed significant increases in the preferred frequency of the first-order Wiener kernel for the following stages: (1) horizontal cell versus on-bipolar cell (0.05 level of significance), (2) horizontal cell versus C amacrine cell (0.05 level), (3) on-bipolar cell versus NB cell (0.0001 level), (4) C amacrine cell versus NB cell (0.0001 level) and (5) NB cell versus NA cell (0.05 level). No significant difference was found between the preferred frequencies of on-bipolar and C amacrine cells. The latter result is significant but not surprising since the dynamic linear system in the Wiener LN (dynamic linear/static nonlinear cascade) model for light-evoked C amacrine output is very similar to the linear system for light-evoked bipolar cell output [7]. The static nonlinearity in the LN model does not affect the shape of the first-order Wiener kernel, which is proportional to the linear system preceding the static nonlinearity [15–18]. Thus the preferred frequency for the C amacrine cell kernel should be the same as that for the

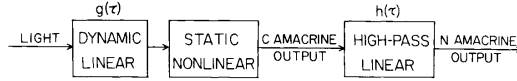


Figure 3. Block diagram for approximating signal processing of light input up to the C amacrine and NB or NA amacrine output stages. The high-pass linear system can explain why the preferred frequency of light-evoked NB or NA first-order kernels is higher than that for the C amacrine cell. The higher preferred frequency for NA than for NB cells suggests that the high-pass system is more sharply differentiating for NA cells.

dynamic linear system in the LN model and therefore very similar to the preferred frequency for the bipolar cell kernel. The simple LN model for the C amacrine cell is, of course, only a first approximation, since the C cell has been shown (H. M. Sakai and K.-I. Naka, unpublished observations) to receive inputs from a variety of cells.

The statistically highly significant increase in preferred frequency from C to N amacrine cells is especially interesting. It jibes well with the proposal of Sakai and Naka [7] of adding a high-pass second linear system (Fig. 3) to convert the C amacrine LN model into the N amacrine LNL (dynamic linear/static nonlinear/dynamic linear cascade) model. The further increase in preferred frequency in penetrating from the NB to the deeper NA level shows a clear difference, and lack of symmetry, in the functional characteristics of the off- and on-amacrine cells. It had earlier been believed that on- and off- pathways were symmetrical, but recently Sakai and Naka [19] have found distinct differences in NB to NA versus NA to NB transmission. The significant difference in preferred frequency which we have now found is further evidence of the breakdown in symmetry between the two pathways.

The hierarchy of preferred frequencies can be summarized as follows:

$$H < (BA, C) < NB < NA,$$

where H and BA denote horizontal cells and on-bipolar cells, respectively. Along this chain, preferred frequency correlated extremely highly ($r = 0.860$) with retinal stage 1 (horizontal cell) through 5 (NA amacrine cell). For a sample size of 44, this correlation is extremely significant ($P < 10^{-7}$).

The linear regression equation relating preferred frequency f to retinal stage s is

$$f = 0.906 + 3.228s. \quad (2)$$

This gives preferred frequencies of 4.13, 7.36, 10.59, 13.82 and 17.06 Hz for horizontal, on-bipolar, C, NB and NA amacrine cells, respectively. Only the predicted preferred frequencies for bipolar and C amacrine cells need be adjusted (towards each other), since no significant difference was found between these two cell classes. Figure 4 shows the scatter diagram for the relation between preferred frequency and retinal stage, together with the linear regression line.

4.4.2. Complexity hierarchies. We found a marked increase in kernel waveform complexity when moving proximally from the NB (off-) amacrine cell to the NA

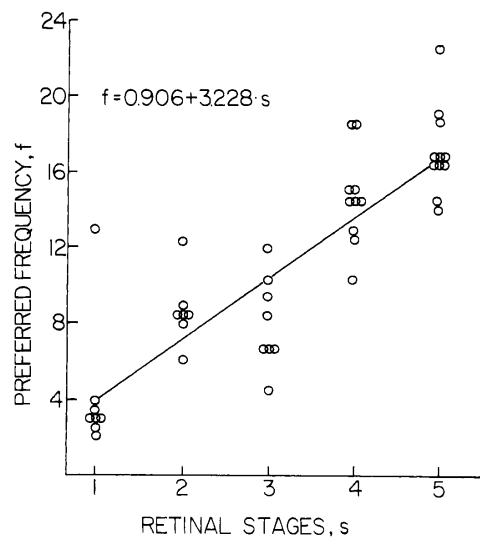


Figure 4. Scatter diagram showing the relationship between the preferred frequency (f), as found by FOS, and five successive retinal stages (s). The linear regression equation is also shown. Correlation coefficient is 0.86 ($P < 10^{-7}$). Stages 1, 2, 3, 4 and 5 correspond to horizontal-, bipolar-, C amacrine, NB amacrine and NA amacrine cell stages.

(on-) cell stage. The increase in complexity was significant at the 0.01 level on both the 3f- and 4f-MSE tests and on the total number of sinusoids selected test. Again (as noted above in respect of preferred frequency), a clear difference between on- and off-cells is revealed. In addition, NA kernel waveform complexity was significantly greater than that for the C cell, on the 4f-MSE test only (about 0.01 level significance).

No significant difference in kernel waveform complexity was found between on-bipolar and horizontal cells, or between on-bipolar and NB cells. However, horizontal cell kernel waveform complexity was significantly less ($P < 0.05$) than that for C amacrine cells, on the total number of sinusoids selected test only. We could also detect an increase in kernel waveform complexity from on-bipolar to C amacrine cells, significant at 0.01 level. This was revealed using the number of sinusoids selected test, but not with the 3f- and 4f-MSE tests. Thus while the preferred frequency does not significantly differ for the latter two cell classes, the waveform for the linear system in the C amacrine LN model is measurably more complex, though similar to, that for the bipolar linear model. Therefore, an increase in kernel waveform complexity was detectable from horizontal to C cells, from on-bipolar to C cells and from C cells to NA cells. Not surprisingly, when either horizontal or on-bipolar cells were

compared directly with NA cells, an increase in kernel waveform complexity was strongly indicated, on all three tests at 0.01 level.

The above noted increases in complexity may be due (see section below on cascade models) to the NA amacrine cell receiving more inputs, or more variety of inputs, than the NB and C cells, while the C cell in turn receives more inputs than do the on-bipolar and horizontal cells. The NB amacrine kernel waveform complexity was also found to be significantly greater ($P < 0.05$) than that of the horizontal cell, on the 4f-MSE test.

However, a very interesting finding was that kernel waveform complexity was greater for the C amacrine (on-off transient) cell than for the NB (off) amacrine cell. This was significant at about the 0.02 level on the total number of sinusoids selected test. Thus waveforms for the signal processing from light input to amacrine cell output appear less complex for NB cells than for C or NA cells. This difference in complexity was also observed in ganglion cells, in our second study.

4.2. Ganglion cells

Our 32 ganglion cell sample comprised 10 GB (off-) cells, 12 GA (on-) cells and 10 GC (on-off) cells. The only significant difference in preferred frequency of kernels was the increase from the GB cells to the GA cells ($P < 0.02$). Thus off-cell kernels are again found to have lower preferred frequencies than on-cells, as we had previously observed for amacrine cells. GB cell kernels also tended to have lower preferred frequencies than on-off cell kernels, but this trend did not reach statistical significance. The differences are less sharp here probably because each type of ganglion cell receives inputs from NB, C and NA amacrine cells, so that a regression toward the mean occurs for ganglion cell preferred frequencies. This is examined further below where we compare preferred frequencies of ganglion cells with those of amacrine cells of the same type.

Much clearer differences were observed in the complexity of kernel waveforms for GB, GA and GC cells. In our ganglion cell sample, there was a correlation of 0.7995 between the 4f-MSE and the total number of sinusoids selected, for a level of significance better than 10^{-4} . The correlation between 3f-MSE and the total number of sinusoids selected was 0.765 ($P < 10^{-4}$). The correlation between 3f- and 4f-MSE was 0.953 ($P < 10^{-4}$). The 3f-MSE test found the kernel waveform complexity of GB cells to be less than that of GA cells (0.02 level significance) which in turn was less than that of GC cells (0.05 level). The 4f-MSE test revealed the same order for kernel waveform complexity, in both comparisons at the 0.05 level. The total number of sinusoids selected test also indicated the same order, at about 0.01 level significance in both comparisons. Thus all three tests find ganglion cell kernel waveform complexity to be ordered:

$$GB < GA < GC.$$

Again the kernel waveforms for signal processing from light input to cell output are less complex for GB cells than for GA or GC cells. Figure 5 illustrates the increasing complexity, as reflected in the number of sinusoids selected, of GB, GA and GC kernels.

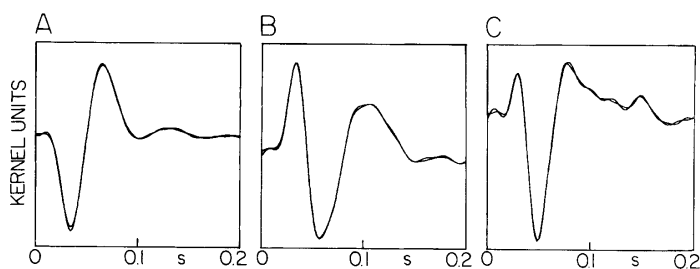


Figure 5. The increase in kernel waveform complexity from the GB (off-center) to the GA (on-center) to the GC (on-off) ganglion cell. For each cell, there are two kernels, one measured experimentally and the other synthesized. (A) The GB cell required eight sinusoidal frequencies to approximate accurately its first-order kernel experimentally measured. (B) The GA cell required 10 sinusoidal frequencies for accurate approximation. (C) The GC cell required 12 sinusoidal frequencies.

4.3. Amacrine cells versus ganglion cells

Finally, we compared preferred frequency and complexity of ganglion cell kernels with that of amacrine cells of same type (i.e. on-, on-off or off-cell). A ganglion cell receives inputs (at least indirectly) from all three types of amacrine cells [6, 7, 20] and a regression towards the mean occurs for the preferred frequencies of ganglion cells. Thus, one might expect that the low preferred frequency of the C amacrine cell would be replaced by a higher preferred frequency in GC cells. This was found to prevail at 0.01 level significance, i.e. for preferred frequency:

$$C < GC.$$

Similarly the higher preferred frequencies of NB, NA cells are replaced by lowered preferred frequencies in the corresponding GB, GA cells:

$$NB > GB,$$

$$NA > GA.$$

The latter two findings were also at the 0.01 level of significance.

Statistically significant differences in kernel waveform complexity were in the same direction as preferred frequency. Thus

$$C < GC,$$

at the 0.05 level of significance on both 3f- and 4f-MSE tests. In addition

$$NA > GA,$$

Table 2.

Relative kernel waveform complexities of horizontal, on-bipolar, amacrine and ganglion cells observed for retinal neurons.

Relative complexity	Level of significance
H < C	0.05
H < NB	0.05
H < NA	0.01
BA < C	0.01
BA < NA	0.01
NB < C	0.02
C < NA	0.01
NB < NA	0.01
GB < GA	0.01
GA < GC	0.01
C < GC	0.05
GA < NA	0.01

Legend: H, horizontal; BA, on-center bipolar; C, on-off amacrine; NB, off-center amacrine; NA, on-center amacrine; GA, on-center ganglion; GB, off-center ganglion; GC, on-off ganglion.

at 0.05 level of significance on 3f-MSE test and at 0.01 level on 4f-MSE test. Kernel waveform complexity differences between NB and GB cells did not reach statistical significance.

The relative kernel waveform complexities of horizontal, on-bipolar, amacrine and ganglion cells are summarized in Table 2.

5. CASCADE MODELS

Many of the results obtained from FOS analysis of first-order kernels from retinal neurons can be appreciated by referring to the cascade model of Fig. 3. This is a block diagram for approximating signal processing of light input up to the C and NB or NA output stages [7]. Sakai and Naka have proposed that the signal processing from light input to C amacrine cell output can be largely accounted for by a particular Wiener (LN) structure in which a (differentiating, dynamic, linear) filter is followed by a static nonlinearity, approximately a squaring device. (The linear component of this nonlinearity is relatively small.) Sakai and Naka [7] also suggest that the light to NB or NA amacrine output relation can be approximated by following the above Wiener structure by a high-pass linear filter, to produce an LNL model. The dovetailing of the C and NB or NA models is shown in Fig. 3 and it will be noted that the high-pass linear filter forms the second dynamic linear system in the LNL model. We show below that this high-pass filter may well explain why the preferred frequency of light-evoked NB or NA first-order kernels is higher than that for the C cell. Moreover, as we shall see, the higher preferred frequency for NA than for NB cells suggests that the high-pass filter is more sharply differentiating for NA cells.

We now consider the amacrine cell light-evoked kernels, i.e. the kernels for the relation between light input and cell output. It can be shown [15–18] that the first-order Wiener kernels for the LN and LNL models are, respectively:

$$k_1(\tau) = A_1 g(\tau), \quad (3)$$

$$K_1(\tau) = B_1 \int_0^{\infty} h(\lambda) g(\tau - \lambda) d\lambda. \quad (4)$$

Here $g(\tau)$ and $h(\tau)$ are the impulse responses of the linear systems, respectively preceding and (in the case of the LNL model) following the static nonlinearity, and A_1 and B_1 are constants.

Similarly, it has been shown [16, 17] that the second-order Wiener kernels for the LN and LNL models are, respectively:

$$k_2(\tau_1, \tau_2) = A_2 g(\tau_1) g(\tau_2), \quad (5)$$

$$K_2(\tau_1, \tau_2) = B_2 \int_0^{\infty} h(\lambda) g(\tau_1 - \lambda) g(\tau_2 - \lambda) d\lambda. \quad (6)$$

Comparing (3) with (4) and (5) with (6) shows that the transition from the LN Wiener kernels to the LNL Wiener kernels is due to convolution with the second linear system of the LNL model. Depending on its characteristics, this second linear system may markedly influence the dynamic properties of the LNL kernels and the changes from the LN kernels will be manifested in the FOS analyses. The effect of the second linear system on the FOS analysis is illustrated below for the first-order kernel, but such effects should also be detectable in higher-order kernels.

First, however, refer again to (3) for the first-order Wiener kernel of the LN structure. As just noted, this LN structure has been used to model accurately the light to C amacrine output relation. Hence it follows from (3) that the shape of the light-evoked first-order kernel of the C cell ought to be the same as that of the linear system preceding the static nonlinearity. In fact, we found the preferred frequency for the C cell did not differ significantly from that for the on-bipolar cell. This is consistent with previous retinal studies, since it has been found that the on-bipolar cell can be accurately represented using a linear system [3, 7, 21] which is similar to the linear system in the LN model for the C amacrine cell.

However, the light-evoked first-order kernel for the NB or NA model is, by (4), proportional to the convolution of the two linear systems in the LNL cascade (Fig. 3). If the second linear system is high-pass, then the first-order NB or NA kernel may have an elevated preferred frequency. This is illustrated in the following example.

We convolved the first-order kernel of a C amacrine cell (Fig. 6A1) with a high-pass linear system (Fig. 6A2). The result, scaled down by a factor of 800, is shown in Fig. 6A3 along with the original first-order kernel. The original kernel of Fig. 6A1 had a preferred frequency of 6.5 Hz (in the lower range for the C cells studied).

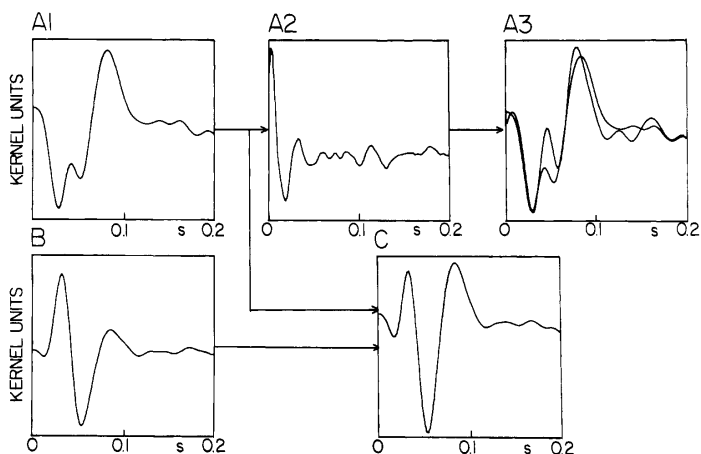


Figure 6. (A) The effect of convolution on the preferred frequency obtained by FOS analysis. The first-order kernel (A1) of a C amacrine cell had a preferred frequency of 6.5 Hz. This kernel was convolved with a high-pass linear system (A2) and the result scaled down by a factor 800 is shown in (A3) (along with the original kernel). The convolution with the high-pass system raised the preferred frequency of the result to 11 Hz. (B and C) The effect of addition of kernels upon complexity as measured by FOS analysis. An NA amacrine first-order kernel (B) was added to the kernel in (A1) to produce the result shown in (C). (A1) and (B) each required nine sinusoidal frequencies for accurate approximation; the sum (C) required 10 sinusoids. (A1) had 3f- and 4f-MSE values of 9.3% and 6.6%, respectively; for (B) the corresponding values were 26.8% and 17.4%. These alternative measures of kernel waveform complexity were elevated in the sum (C) which had 3f- and 4f-MSE values of 35% and 24.8%, respectively.

The convolved result had a preferred frequency of 11 Hz. (However, convolution did not increase the number of sinusoids required to accurately represent the kernel: the original kernel required nine sinusoids and the convolved result required only eight sinusoids.)

Hence, as shown in this example, having a high-pass system in the cascade may well raise the preferred frequency of the first-order kernel, and so explains why the NA and NB amacrine cells tend to have higher preferred frequencies than C amacrine cells. Thus, in some cases, preferred frequency can reflect the number of stages in the cascade or chain leading up to the output of a cell.

As noted, we have found that NA cells tend to have higher preferred frequencies than NB cells (see also below). This suggests that the high-pass linear system following the static nonlinearity (Fig. 3) is more sharply differentiating for the NA cells.

Next, consider kernel waveform complexity, measured, for example, by the mean-square error remaining after best-fitting with the most significant three or four sinusoids (the 3f- or 4f-MSE). An alternate measure of complexity is the number of sinusoids selected, until no further choice could reduce the mean-square error by more

than 0.2% of the time-series variance. This criterion always resulted in an excellent fit of the kernel. Here we illustrate that receiving inputs from two or more cells can increase kernel waveform complexity. Indeed, it is hardly surprising that receiving multiple inputs can complicate the measured kernels, especially if the inputs are from different kinds of neurons. In this case, a wide variety of sinusoidal frequencies may be introduced into the measured kernel.

We added the first-order kernel of an NA amacrine cell (Fig. 6B) to that of the C cell (Fig. 6A1). The sum is shown in Fig. 6C. The C and NA amacrine first-order kernels each required nine sinusoids for accurate representation according to the 0.2% criterion discussed above. The sum required 10 sinusoids. The C and NA kernels had 3f-MSE values of 9.3% and 26.8%, respectively; the sum (Fig. 6C) had a 3f-MSE of 35%. The corresponding values of 4f-MSE were 6.6%, 17.4% and 24.8%. (The preferred frequency of the sum, i.e. 13.5 Hz, showed a slight tendency to regress toward the mean of the preferred frequencies of the C cell, i.e. 6.5 Hz, and the NA cell, i.e. 14 Hz.)

While this example shows that receiving multiple inputs can complicate the first-order kernel, it may generally require far more than two inputs to significantly increase kernel waveform complexity. Indeed, with the tremendous interconnectivity of the neural network [19] it is noteworthy that 14 sinusoids were the most ever required to achieve a better than 99% fit of the first-order kernel. This number was required only once, by an NA amacrine cell, out of 76 neurons studied. The limited number of sinusoids required to accurately represent the kernels may be one of the reasons that the sum-of-sinusoids approach [22, 23] has been so successful in neurophysiology.

6. DISCUSSION

The extreme interconnectivity of neurons in the vertebrate outer and inner retina has rendered their individual functional characteristics very difficult to decipher. It has however provoked development and use of the white-noise approach [24–30] to study the signal processing in a complex biological system. In particular, Wiener's [24] statistical theory of nonlinear system identification shows that any time-invariant continuous finite-memory nonlinear system belonging to a very wide class can be fully identified from knowledge of its response to a white Gaussian input. The system is identified by measuring the Wiener kernels, which comprise a constant, and one- and multi-dimensional weighting functions.

A related approach to nonlinear system identification utilizes cascade or block-structured models. One frequently-used structure is the cascade of a dynamic linear, a static nonlinear and a dynamic linear component, an 'LNL cascade'. Spekreijse [31] and Spekreijse and Oosting [18] demonstrated that, once a suitable template library had been prepared, the individual components of the LNL cascade could be identified using multiple runs of certain test input signals. This identification was possible in their method provided that the static nonlinearity could be recognized by comparing some calculated characteristics for it with those from a previously prepared library of studied nonlinearities. Korenberg [16, 17] showed how the LNL cascade could be 'completely' identified from a single white-noise experiment in a general

method. (The LNL cascade components are identifiable up to arbitrary proportionality constants and a phase shift.) Subsequently, a simple time-domain identification was presented and the LNL cascade was generalized to multi-input, multi-output systems [32, 33]. Two subclasses of the LNL cascade are the Wiener (LN) dynamic linear/static nonlinear structure and the Hammerstein (NL) static nonlinear/dynamic linear structure [34].

Certain tests for the Wiener, Hammerstein and LNL cascade structures have been set down [16, 17, 34, 35] which involve the system's Wiener kernels or equivalent input output cross-correlations. These conditions serve to illustrate what can be learned about a system by studying its Wiener kernels. Recently, cascade identification has been used to study neural encoding by an insect mechanoreceptor [36, 37].

In the case of the catfish retina, these cascade structures were suggested as being appropriate models from a study of the first- and second-order Wiener kernels characterizing the relationship between the white Gaussian input light and amacrine cell output. For example, the second-order Wiener kernel is a two-dimensional function and its contour plot, for light input to C amacrine cell output relation, has a characteristic three- or four-eye appearance [7, 38]. This contour plot can be readily reproduced [7, 38] by using two-dimensional multiplication of the first-order kernel (a one-dimensional function) and therefore satisfies a necessary condition [16] for the Wiener structure of a dynamic linear/static nonlinear cascade. (In carrying out this two-dimensional multiplication, one can replace the first-order kernel with a slice of the second-order kernel parallel to one axis and this was done [7, 38] because the C cell first-order kernel is very small.) On the other hand, the second-order kernel contour plot for the NA or NB amacrine cell is reproducible [7, 38] if the above Wiener structure is followed by a brief-duration differentiating, or high-pass, linear system. This explains the above-noted proposal [7, 38] of a dynamic linear/static nonlinear/dynamic linear model for the light input to NA or NB output relationship. Formal methods are available [16, 17, 32, 33] for identifying the components of such an LNL cascade and are currently being utilized in our work. Recently, cascade analysis was further used [39] to provide an explanation for the strong similarity, as well as slight discrepancy, between light-evoked slow potential kernels and spike kernels of ganglion cells. This remarkable similarity, and slight discrepancy, between the two sets of kernels had previously been observed by Sakuranaga *et al.* [38] and by Sakai and Naka [7].

In this paper we have also made use of a recently invented technique, FOS [8, 9], to probe the retinal network. FOS enables a precise analysis of the frequency content of a signal, frequently more than eight times the accuracy of the DFT. This increased resolution (here, we utilized 0.5 Hz resolution as opposed to 3.906 Hz for the DFT) directly led to some new findings. For instance, it enabled us to measure accurately the small increase from NB amacrine preferred frequency, averaging 14.65 Hz, to NA preferred frequency, averaging 17.18 Hz. FOS has also delineated in detail a frequency hierarchy for the horizontal, on-bipolar, C, NB and NA amacrine cells. Moreover, the clear difference in preferred frequency between on- (NA) and off- (NB) cells was again found between on- (GA) and off- (GB) ganglion cells. In both cases, the kernels of on-cells tend to have higher preferred frequencies than those of

off-cells. FOS has in addition enabled us to study the complexity of the waveforms of retinal cell kernels. Again, for both amacrine and ganglion cells, a clear difference was found between the on- and the off-cells, with on-cells having significantly more complex kernel waveforms than off-cells.

We will now discuss some of the major conclusions of the above FOS analysis in relationship to the morphology and physiology of the catfish retinal neuron network.

(1) FOS analysis has found a progressive increase in the preferred frequency from the horizontal to N amacrine cells. Although past analysis in the form of the Fourier transform of the first-order kernels tends to suggest this trend, no accurate quantitative definition of this trend was possible. The frequency response of the horizontal cells [3] is from DC to less than 10 Hz (defined by the -3 dB point) and the present study has shown that the cell's preferred frequency is about 4 Hz. Although our data on the receptors are not as extensive, their frequency response is similar to that for the horizontal cells. We believe it is through the introduction of band-pass or high-pass filters (which follow static nonlinearities) that the preferred frequency is increased to about 17 Hz in the NA amacrine cell. These higher frequency components in the amacrine cell responses enable such neurons to respond to higher frequency components in the light input. These components also facilitate initiation of spike discharges in the ganglion cells. This important aspect of network mechanism has not previously been given much attention. One exception is the study by Baylor and Fettiplace [2], in which they showed that ganglion cells had kinetics faster than the receptors.

(2) The kernel for the NA amacrine cell has a preferred frequency higher than that for the NB cell. As noted above, this difference suggests that the high-pass linear system in the cascade model for the NA cell is more sharply differentiating than the corresponding system for the NB cell. This difference can be appreciated by noting that there are faster first-order kernels from NA than from NB cells (Fig. 8 in [6]). It has previously not been possible, though, to study the frequency responses with high resolution and to measure accurately subtle frequency response differences between NA and NB cells. The difference in the second linear filter may also account for the difference observed in the second-order kernels from NA and NB cells (Fig. 9 in [6]).

(3) Bipolar and C amacrine cells have similar preferred frequencies. Although the Wiener model for the C amacrine cell would imply this conclusion, no experimental evidence was available because of the frequency doubling characteristics of the C cell and because of noisy estimates of its small first-order kernel. Due to this noise, previous analysis of the C kernel using the DFT was not successful whereas FOS gave consistent results. The fact that both bipolar and C cells have similar preferred frequencies is an important finding because it shows that the increase in the preferred frequency takes place in the N amacrine cell but not in the C cell. Production of a faster linear component may be one of the functions of N amacrine cells.

(4) Complexity of the kernel waveform increased from horizontal to N amacrine cells. Although this fact was intuitively appreciated, no quantitative measurement was possible.

(5) NA amacrine cells possessed a kernel waveform more complex than that of NB amacrine cells. Our past results failed to detect this difference. We have found that NA amacrine cells are located in the proximal layer of the inner plexiform layer (IPL) whereas NB cells are located in the distal layer. This morphological asymmetry may be related to the functional asymmetry we observed here.

(6) The on-ganglion cell kernel waveform is less complex than that for the NA amacrine cell kernel. With hindsight, this is what one would expect from the fact that ganglion cells receive direct inputs from bipolar cells. However, virtually no evidence was available on this point, except for the observation that ganglion cell responses have larger linear components than amacrine cell responses [7].

(7) There is a difference in complexity of kernel waveforms for GC, GA and GB ganglion cells, similar to that for C, NA and NB amacrine cells. For both amacrine and ganglion cells, kernel waveforms of off-cells are less complex than those of both on-off and on-cells. Past studies have failed to detect these differences. FOS analysis indicated that kernel waveform complexity increased from GB to GA to GC ganglion cells. In the model of neuron circuitry proposed for the catfish retina (Fig. 20 in [7]; Fig. 11 in [19]), the direct pathway leading to the GC cells involves a fewer number of synapses than for GB or GA cells. However, GC cells also receive inputs from on- and off-pathways (as evidenced by GC cells' linear components) in addition to inputs from on-off pathways. The GA and GB cells, on the other hand, receive exclusively inputs from on- and off-pathways, respectively (at least directly). Hence, GC cells probably receive a greater variety of inputs than do the other two ganglion cell types. Although the circuitry proposed for GA and GB cells is symmetric, we observed consistently that the responses from GA cells were found in the proximal layer of IPL, whereas those from GB cells were found in the distal layer (as in the case of N amacrine cells). Again this morphological difference may be related to the difference in complexity of kernel waveforms we discovered here. In other species morphological segregation of the on- and off-pathways was observed.

Thus results obtained in this paper provide a set of independent evidence that corroborates some of the network mechanisms we proposed for the catfish retina.

Moreover, there is very extensive communication between cells, such as ganglion-ganglion, ganglion-amacrine and amacrine-amacrine transmission, and this communication exists within and between on-, off- and on-off pathways [19, 40]. The wide variety of inputs received by a cell increases the complexity of the first- and higher-order light-evoked kernel waveforms measured for the cell. FOS has now been used to quantify the kernel waveform complexity for signal processing from light input to a given cell output.

These new facts uncovered by the FOS method indicate that there are much more subtle differences in the responses from various neurons in the catfish retina and these subtle differences may indicate equally subtle differences in the signal processing performed by retinal neurons. The picture one can make of the retinal circuitry depends on the power and precision of the analytical tool one applies to analyze the circuitry: this is not at all surprising if one considers the extremely complex synaptic structure of the retina, especially that of the inner retina.

Acknowledgements

The authors thank the reviewers for their astute comments on the manuscript. This research was supported partly by the Natural Sciences and Engineering Research Council of Canada, the National Eye Institute grants NEI 07738 (PI, K.-I.N.), NEI08847 (PI, H.M.S.), and the National Institute of Neurological Diseases and Stroke NS30722. K.-I.N. also thanks Research to Prevent Blindness for his Jules and Doris Stein Professorship.

REFERENCES

1. F. S. Werblin and J. E. Dowling. Organization of the retina of the mudpuppy, *Necturus maculosus*. II. Intracellular recording. *J. Neurophysiol.* **32**, 339–354 (1969).
2. D. A. Baylor and R. Fettiplace. Kinetics of synaptic transfer from receptors to ganglion cells in turtle retina. *J. Physiol.* **271**, 425–448 (1977).
3. M. Sakuranaga and K.-I. Naka. Signal transmission in the catfish retina. I. Transmission in the outer retina. *J. Neurophysiol.* **53**, 373–389 (1985).
4. M. Sakuranaga and K.-I. Naka. Signal transmission in the catfish retina. II. Transmission to type-N cell. *J. Neurophysiol.* **53**, 390–410 (1985).
5. M. Sakuranaga and K.-I. Naka. Signal transmission in the catfish retina. III. Transmission to type-C cell. *J. Neurophysiol.* **53**, 411–428 (1985).
6. H. M. Sakai and K.-I. Naka. Signal transmission in the catfish retina. IV. Transmission to ganglion cells. *J. Neurophysiol.* **58**, 1307–1328 (1987).
7. H. M. Sakai and K.-I. Naka. Signal transmission in the catfish retina. V. Sensitivity and circuit. *J. Neurophysiol.* **58**, 1329–1350 (1987).
8. M. J. Korenberg. Fast orthogonal identification of nonlinear difference equation and functional expansion models. *Proc. Midwest Symp. Circuit Sys.* **1**, 270–276 (1987).
9. M. J. Korenberg. A robust orthogonal algorithm for system identification and time-series analysis. *Biol. Cybern.* **60**, 267–276 (1989).
10. K. M. Adeney and M. J. Korenberg. Fast orthogonal search for direction finding. *Electron. Lett.* **28**, 2268–2269 (1992).
11. K. M. Adeney and M. J. Korenberg. Fast orthogonal search for array processing and spectrum estimation. *IEEE Proc. Vis. Image Sig. Process.* **141**, 13–18 (1994).
12. W. H. Press, B. P. Flannery, S. A. Teukolsky and W. T. Vetterling. *Numerical Recipes in C: The Art of Scientific Computing*. Cambridge University Press, Cambridge (1988).
13. M. G. F. Fuortes and A. L. Hodgkin. Changes in time scale and sensitivity in the ommatidia of limulus. *J. Physiol.* **172**, 239–263 (1964).
14. R. M. Shapley and J. D. Victor. How the contrast gain control modifies the frequency response of cat retinal ganglion cells. *J. Physiol.* **318**, 161–179 (1981).
15. J. J. Busgang. Crosscorrelation functions of amplitude-distorted Gaussian signals. *MIT Res. Lab. Elec. Tech. Rep.* **216**, 1–14 (1952).
16. M. J. Korenberg. Identification of biological cascades of linear and static nonlinear systems. *Proc. Midwest Symp. Circuit Theory* **18.2**, 1–9 (1973).
17. M. J. Korenberg. Cross-correlation analysis of neural cascades. *Proc. Ann. Rocky Mountain Bioengin. Symp.* **1**, 47–52 (1973).
18. H. Spekreijse and J. Oosting. Linearizing: a method for analyzing and synthesizing nonlinear systems. *Kybernetik* **74**, 23–31 (1970).
19. H. M. Sakai and K.-I. Naka. Dissection of the neuron network in the catfish inner retina. V. Interactions between NA and NB amacrine cells. *J. Neurophysiol.* **63**, 120–130 (1990).
20. H. M. Sakai and K.-I. Naka. Dissection of the neuron network in the catfish inner retina. I. Transmission to ganglion cells. *J. Neurophysiol.* **60**, 1549–1567 (1988).

21. K.-I. Naka, P. Z. Marmarelis and R. Y. Chan. Morphological and functional identifications of catfish retinal neurons. III. Functional identification. *J. Neurophysiol.* **38**, 92–131 (1975).
22. J. D. Victor and B. W. Knight. Nonlinear analysis with an arbitrary stimulus ensemble. *Q. Appl. Math.* **37**, 113–136 (1979).
23. J. D. Victor and R. M. Shapley. The nonlinear pathway of Y ganglion cells in the cat retina. *J. Gen. Physiol.* **74**, 671–687 (1979).
24. N. Wiener. *Nonlinear Problems in Random Theory*. Wiley, New York (1958).
25. Y. W. Lee and M. Schetzen. Measurement of the Wiener kernels of a nonlinear system by cross-correlation. *Int. J. Control* **2**, 237–254 (1965).
26. P. Z. Marmarelis and K.-I. Naka. White-noise analysis of a neuron chain: an application of the Wiener theory. *Science* **175**, 1276–1278 (1972).
27. P. Z. Marmarelis and V. Z. Marmarelis. *Analysis of Physiological Systems. The White-Noise Approach*. Plenum Press, New York (1978).
28. M. Sakuranaga, S. Sato, E. Hida and K.-I. Naka. Nonlinear analysis: mathematical theory and biological applications. *Crit. Rev. Biomed. Eng.* **14**, 127–184 (1986).
29. H. M. Sakai, K.-I. Naka and M. J. Korenberg. White-noise analysis in visual neuroscience. *Vis. Neurosci.* **1**, 287–296 (1988).
30. M. J. Korenberg and I. W. Hunter. The identification of nonlinear biological systems: Wiener kernel approaches. *Ann. Biomed. Engng.* **18**, 629–654 (1990).
31. H. Spekreijse. Rectification in the goldfish retina: analysis by sinusoidal and auxiliary stimulation. *Vis. Res.* **9**, 1461–1472 (1969).
32. M. J. Korenberg. Statistical identification of parallel cascades of linear and nonlinear systems (Preprints). *IFAC Symp. Ident. Sys. Param. Est.* **1**, 580–585 (1982).
33. M. J. Korenberg. Identifying noisy cascades of linear and static nonlinear systems (Preprints). *IFAC Symp. Ident. Sys. Param. Est.* **1**, 421–426 (1985).
34. I. W. Hunter and M. J. Korenberg. The identification of nonlinear biological systems: Wiener and Hammerstein cascade models. *Biol. Cybernet.* **55**, 135–144 (1986).
35. M. J. Korenberg and I. W. Hunter. The identification of nonlinear biological systems: LNL cascade models. *Biol. Cybernet.* **55**, 125–134 (1986).
36. M. J. Korenberg, A. S. French and S. K. L. Voo. White-noise analysis of nonlinear behaviour in an insect sensory neuron: kernel and cascade approaches. *Biol. Cybernet.* **58**, 313–320 (1988).
37. A. S. French and M. J. Korenberg. A nonlinear cascade model for action potential encoding in an insect sensory neuron. *Biophys. J.* **55**, 655–661 (1989).
38. M. Sakuranaga, Y.-I. Ando and K.-I. Naka. Dynamics of ganglion cell response in the catfish and frog retinas. *J. Gen. Physiol.* **90**, 229–259 (1987).
39. M. J. Korenberg, H. M. Sakai and K.-I. Naka. Dissection of the neuron network in the catfish inner retina. III. Interpretation of spike kernels. *J. Neurophysiol.* **61**, 1110–1120 (1989).
40. H. M. Sakai and K.-I. Naka. Dissection of the neuron network in the catfish inner retina. IV. Bidirectional interactions between amacrine and ganglion cells. *J. Neurophysiol.* **63**, 105–119 (1990).